DOI: http://dx.doi.org/10.32571/ijct.1661831 **E-ISSN: 2602-277X**

International Journal of Chemistry and Technology

http://dergipark.org.tr/ijct

Research Article

Structural and Electronic Properties of Double Transition Metal Mo_2MC_2X (M = Mn, W; X = O_2, S_2, OS) MXenes

Sibel ÖZCAN[1*]

[1*]*Department of Physics, Aksaray University, 68100, Aksaray, Turkey*

Received: 20 March 2025; Revised: 27 May 2025; Accepted: 12 June 2025

*Corresponding author e-mail: sozkaya@aksaray.edu.tr

Citation: Özcan, S**.** *Int. J. Chem. Technol.* **2025**, 9(1), 134-139

ABSTRACT

MXenes are gaining importance for their novel properties and interesting behaviors. In this study, based on the pseudopotential method and density functional theory, we present that the 35 feasible members of the Janus Mo_2MC_2X (M = Mn, W; X = O_2, S_2, OS) family with seven possible structural models (i) AA', (ii) AB', (iii) AC', (iv) BB', (v) BC', (vi) CB', (vii) CC', are all stable. The calculation results of the structural and elastic properties (elastic constants, Poisson's ratio, Young modulus, etc.) show that the Mo_2MC_2X is stronger than the other 2D monolayers such as graphene. The $Mo_2WC_2S_2$ is a valuable candidate for flexible electronics and highly sensitive resonating mass sensors due to its very high Young's modulus. The calculated electronic band structures of considered MXenes are metallic. Our findings are anticipated to encourage the development of MXene-based devices.

Keywords: Janus MXenes, surface functionalization, density functional theory.

1. INTRODUCTION

The two-dimensional (2D) early transition metal (TM) carbides and nitrides (MXene) have drawn growing research interest owing to their extensive applications, such as in sensors,[1,2] energy storage,[3-8] catalysis[9] electromagnetism,[10-13] and other fields.[14] The general formula of MXenes is $M_{n+1}X_n$, where M corresponds the transition metal (Ti, V, Nb, Ta, Cr, Mo, etc.), X represents C or N, and n = 1, 2, or 3.[15,16] The surface of the MXenes can be easily passivated by diverse functional groups, and the general formula for them is $M_{n+1}X_nN_x$, where N denotes the terminating atoms[17]. Besides the fluorine, oxygen, and hydroxyl functionalized groups,[18,19] the surface terminations, including NH, S, Cl, Se, Br, and Te, were synthesized and show original structural and electronic properties.[20] While experimental and theoretical investigations reported that pristine MXenes are metallic, the functionalization of MXenes by various functional groups changes their electronic properties to semiconducting, for instance, Hf_2CO_2, Sc_2CO_2, $Sc_2C(OH)_2$, Sc_2CF_2, Ti_2CO_2, and Zr_2CO_2[21- 24]. Besides the impact on the electronic structure, the functional groups play critical roles in the assorted properties of MXenes, such as the electronic and thermal transport, thermodynamic stability, and elasticity of the MXenes[25-28]. For example, the diffusion barrier of the S-terminated surface is lower than their O-functionalized counterparts,[29,30] which is crucial data for the adequate electrode material for batteries.

The double TM 2D carbide MXenes ($M_2'M''C_2$) have two different TM atoms M'(occupy outer layers) and M''(fill the centeral layers). Recently, the double TM 2D carbide MXenes, such as $Mo_2TiC_2T_x$, $Mo_2Ti_2C_3T_x$, and $Cr_2TiC_2T_x$, were also synthesized and validated with the DFT predictions.[31,32] Wang et al. demonstrated that the pristine Mo_2MC_2 (M = Sc, Ti, V, Zr, Nb, Hf, Ta) and surface terminated $Mo_2MC_2T_2$ (T = H, O, F, and OH) are convenient for use in lithium-ion batteries (LIBs) as an anode material.[33]

DOI: http://dx.doi.org/10.32571/ijct.1661831 E-ISSN: 2602-277X

In Janus structure, the two different chemical surfaces (i.e., two surfaces of material have other functional groups) break the mirror symmetry of the system, introducing an out-of-plane-structural symmetry, which can make Janus structure special features such as an intrinsic out-of-plane electric field.[34]

Following experimental attainments of Janus monolayers of TM dichalcogenides,[35,36] the synthesis of Janus MXenes is expected. The previous report has theoretically shown that the energy gap of Janus MXenes, containing Cr_2C (Cr_2CXX', X, X' = H, F, Cl, Br, OH) and V_2CFOH, can be arranged by choosing suitable functional elements.[37] Liu et al. demonstrated that the electronic structure of Hf_2CO_2 changed from a semiconductor to metal Hf_2COT (T = -Br, -Cl, –F, –OH, -P, –S, -Se) when terminating the atoms asymmetrically.[38]

Understanding the structural and electronic properties of MXene-based materials is necessary for designing devices and advancements of these systems. This study aims to contribute knowledge by studying all available 2D Janus systems based on the Mo_2MC_2X (M = Mn, W, X = O_2, S_2, OS) MXenes through DFT approaches.

2. METHODS

Our calculations were performed within Density Functional Theory (DFT) using the Vienna Ab initio Simulation Package (VASP).[39-43] The electron wave functions are expanded based on a plane wave basis set up to the cut-off energy of 30 Ry. The broadening width is set to 0.05 eV with the Fermi level Gaussian smearing methods. The valence electrons and the core interactions were described using the projector augmented-wave (PAW) method.[43,44] For electron exchange and correlation terms, the generalized gradient approximation (GGA)[44] in its Perdew-Burke- Ernzerhof (PBE)[45] functional parametrized by Perdew–Zunger[45,46] was adopted. Our calculations were refined using the Heyd–Scuseria–Ernzerhof (HSE06) functional, which has been proven to yield energy band gaps. To facilitate Brillouin zone integration, we obtain the Self-consistent solutions using the (15×15×2) Monkhorst–Pack47 mesh of k-points. A vacuum layer of more than 10 Å was included for each considered structure to avoid any possible artificial interactions arising from periodic boundary conditions. The stress-strain approach[48] was used to calculate the elastic tensor of each MXene.

3. RESULTS and DISCUSSION

Mo_2MC_2 (M = Mn, W) has a hexagonal structure with space group symmetry $Pm1\bar{3}$ (space group number 164). Before studying functional groups on Mo_2MC_2 (M = Mn, W) MXene, all structures were fully relaxed. The lattice constant of the relaxed unit cell is 2.96 (3.04) Å for the Mo_2MnC_2 (Mo_2WC_2). These results are comparable with the earlier theoretical studies that the lattice constants of Mo_2TiC_2, Mo_2TaC_2, and Mo_2VC_2 are 2.97, 3.02, and 2.94 Å, respectively.[49] After getting the ground state crystal structure of pristine Mo_2MC_2 (M = Mn, W), we continued the functionalization of Mo_2MC_2 (M: Mn, W) MXene monolayer with X = O, S, and OS. We considered seven configurations of O, and S atoms according to the relative positions of the functional groups attached to the top and the bottom of the Mo_2MC_2 (M = Mn, W) surface. As presented in Figure 1, we labeled A (aligned with the M atom), B (aligned with the Mo atom), C (aligned with the C atom) for the top of the surface, and A', B', C' for the bottom of the surface. For example, in the CB' model of Mo_2MC_2OS (M = Mn, W) MXene, the O atom sits on the C, and the S atom is under the B'. AA', AB', AC', BB', CB', BC', and CC' type positions were optimized to get the most stable model. We have calculated the relative total energies concerning the most stable model for each structure (ΔE) and tabulated them in Table 1. We will concentrate on this geometry since the most stable model is CB.

To assess the stability of all the structures, formation energies (Ef) are calculated as below equations (1, 2):

$$Ef = E_{Mo_2MC_2OS} - E_{Mo_2MC_2} - E_O - E_S \quad (1)$$

$$Ef = E_{Mo_2MC_2Y_2} - E_{Mo_2MC_2} - 2E_Y \quad (2)$$

where $E_{Mo_2MC_2OS}$, $E_{Mo_2MC_2Y_2}$ (Y = O or S), $E_{Mo_2MC_2}$, E_O, and E_S ($E_Y = E_O$ *or* E_S) are the total energy of the surface terminated Mo_2MC_2OS (M = Mn, W), $Mo_2MC_2O_2$, or $Mo_2MC_2S_2$, the total energy of pristine Mo_2MC_2, and the total energy of (1/2) O_2 (gas molecule), and S (stable bulk form), respectively. As shown in Table 2, all the considered models' formation energies are negative, which means synthesizing these MXenes is extremely feasible (we represented more negative formation energy, which denotes a more stable structure). The investigation of the Born criteria we present below also confirmed the stability of these MXenes.

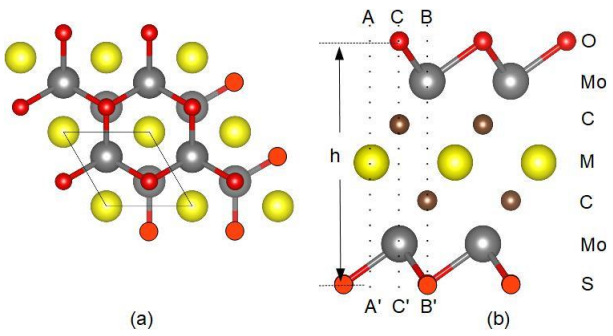

Figure 1. (a) Top and (b) side views of the Mo_2MC_2OS (M = Mn, W) (CB' model). We only exhibit the Mo_2MC_2OS structure because the only change concerning $Mo_2MC_2O_2$ ($Mo_2MC_2S_2$) is that the top and bottom layers have different atoms instead of two same atoms.

DOI: http://dx.doi.org/10.32571/ijct.1661831 **E-ISSN: 2602-277X**

Table 1. Relative energies concerning the minimum energy for each model ΔE (in eV) for the Mo_2MC_2X (M = Mn, W; X = O, S, OS) in the seven possible models.

Material	AA'	AB'	AC'	BB'	BC'	CB'	CC'
$Mo_2MnC_2O_2$	0.96	0.36	2.00	1.43	3.00	0.00	1.45
$Mo_2MnC_2S_2$	1.04	0.52	2.09	1.60	3.23	0.00	1.60
Mo_2MnC_2OS	0.97	0.42	2.13	1.43	3.14	0.00	1.60
$Mo_2WC_2O_2$	0.76	0.36	4.27	0.98	0.99	0.00	2.67
$Mo_2WC_2S_2$	1.15	0.55	3.44	6.50	3.34	0.00	1.43
Mo_2WC_2OS	0.98	0.42	2.48	2.40	2.81	0.00	4.55

Due to the transition of electrons from Mo atoms to X (O or S), the Mo-X bond strengthens, and the Ef becomes more negative. As seen in Table 1, the $Mo_2MC_2O_2$ (M = Mn, W) has a shorter Mo-O bond length (a strong Mo–O interaction) and more negative Ef. The Mo_2MnC_2OS structure is more stable than $Mo_2MnC_2S_2$, which can be explained by the increasing electronegativity of functional atoms (O more electronegative than S) becoming more negative Ef. The thickness of the $Mo_2MnC_2O_2$ (7.33 Å) is close to that of $Mo_2WC_2O_2$ (7.77 Å), evidenced that the center layer of the Mo_2MC_2X (M = Mn, W; X = O, S, OS) MXenes has a negligible effect on the thickness. The distance between the Mo-O atoms is shorter than the Mo-S bond length. Consequently, the monolayer thickness of $Mo_2MC_2O_2$ (M = Mn, W) is shorter than the other considered MXenes.

Table 2. Calculated monolayer thickness (h (Å)), bond lengths between the Mo and the functional groups (d(Mo–X (Å) (d(Mo-X') (Å) for X≠X')), and formation energies Ef (in eV) of Mo_2MC_2X (M = Mn, W; X = O, S, OS) MXenes.

Material	h	d(Mo-X) (d(Mo-X') for X≠X')	Ef
$Mo_2MnC_2O_2$	7.33	2.10	-7.43
$Mo_2MnC_2S_2$	8.21	2.39	-4.38
Mo_2MnC_2OS	7.77	2.10 (d(Mo-S)= 2.39)	-5.93
$Mo_2WC_2O_2$	7.60	2.12	-7.05
$Mo_2WC_2S_2$	8.50	2.41	-4.64
Mo_2WC_2OS	8.04	2.12 (d(Mo-S)= 2.41)	-5.88

The mechanical properties of 2D materials are crucial for 2D nanodevice design. For this reason, the elastic properties of this MXene family have been studied according to the Born criteria[50] (Equation 3) as follows;

"$C_{11}>0$, $C_{66}>0$, $2*C_{66}= C_{11}-C_{12}$, and $C_{11} >|C_{12}|$" (3)

As seen in Table 3, all MXenes satisfy the Born criteria, which implies that they are mechanically stable.

We also calculated Young's modulus Y, Poisson's ratio ν, and the shear modulus G, derived from the elastic constants of considered MXenes for understanding other mechanical properties,[51-53] as below:

"$Y = (C_{11}-C_{12})/C_{11}$,
$\nu = C_{12}/C_{11}$, (4)
$G = (C_{11}-C_{12})/2$"

and tabulated in Table 3. The Young modules of the $Mo_2WC_2X_2$ MXenes are higher than those of $Mo_2MnC_2X_2$, demonstrating that the middle layer affects mechanical strength for our considered MXenes. The $Mo_2WC_2S_2$ has the highest in-plane Young's module of 481.311 Nm^{-1}, which means this crystal is stiffer than the materials considered in this study. We have calculated the Y values within the range of 355.066 and 481.311 Nm^{-1}. These values are higher than that of graphene (341 N m^{-1}),[54,] which indicates a strong mechanical strength, and other 2D materials such as silicene (62 Nm^{-1})[55] and germanene (44 Nm^{-1}).[55] The ultrahigh Young's modulus values make Mo_2MC_2X (M = Mn, W; X = O_2, S_2, OS) MXenes an ideal candidate for flexible electronic applications.

The Poisson's ratios of the Mo_2MC_2X (M=Mn, W; X=O_2, S_2, OS) MXenes studied here range from 0.307 to 0.396, indicating the ductility of these materials, and are comparable with the values obtained for MoS_2 (0.25),[54] germanene (0.33),[55] stanene (0.39).[55]

Table 3. Elastic constants (C_{ij} in Nm^{-1}), young's moduli (Y in Nm^{-1}), shear moduli (G in Nm^{-1}), and poisson's ratios (ν).

Material	C_{11}	C_{12}	C_{66}	Y	G	ν
$Mo_2MnC_2O_2$	421.213	166.919	127.147	355.066	127.147	0.396
$Mo_2MnC_2S_2$	516.077	186.922	164.577	448.374	164.577	0.362
Mo_2MnC_2OS	469.977	178.242	145.868	402.378	145.868	0.379
$Mo_2WC_2O_2$	449.588	153.002	148.293	397.519	148.293	0.340
$Mo_2WC_2S_2$	531.501	163.327	184.087	481.311	184.087	0.307
Mo_2WC_2OS	493.645	159.748	166.948	441.949	166.948	0.324

DOI: http://dx.doi.org/10.32571/ijct.1661831 **E-ISSN: 2602-277X**

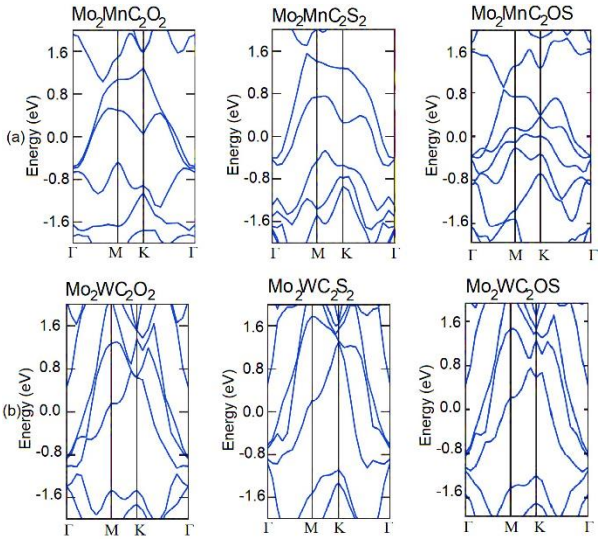

Figure 2. Band structures for the most stable models of (a) Mo_2MnC_2X and (b) Mo_2WC_2X monolayers (X = O_2, S_2, OS). The Fermi level is set at zero.

To further understand the effect of O- and S- atom functionalization and middle layer atom of the Mo_2MC_2X (M = Mn, W) MXene, their band structures and partial density of states (PDOS) are calculated and plotted in Figures 2 and 3, respectively. While the previous reports show that functionalization can cause a changing the electronic properties (metal to semiconductor) such as Ti_2CO_2, Zr_2CO_2, Hf_2CO_2, Sc_2CO_2, $Sc_2C(OH)_2$, and Sc_2CF_2,[21-24] as seen in Figure 2, Mo_2MC_2X (M = Mn, W; X=O_2, S_2, OS) MXenes show metallic behavior.

Similarly, a previous report illustrated that the band structures of the $M_2M'C_2T_2$ (M = Cr, Mo; M'= Ti, V) MXenes are metallic.[56]

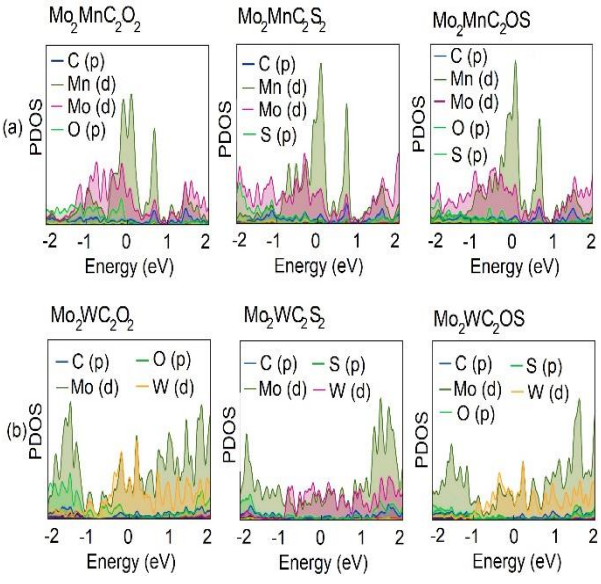

Figure 3. Calculated Projected Density of States (PDOS) of (a) Mo_2MnC_2X and (b) Mo_2WC_2X monolayers (X = O_2, S_2, OS). The Fermi level is set at zero.

The PDOS presented in Figure 3 reveals valuable information about the contribution of specific electronic states of these materials. While the states around the Fermi level are mainly contributing from the Mn (d) atom for Mo_2MnC_2X (X = O_2, S_2, OS), the metallicity primarily derived from the d orbitals of the W and Mo atoms for Mo_2WC_2X (X = O_2, S_2, OS). The d orbital of the Mo atoms induced to the states above the Fermi level (EF) (between 1 and 2 eV) and below the EF (between -1 and -2 eV).

4. CONCLUSION

In the presented work, based on first-principles computations, a systematic computational study has been carried out to investigate the structural, elastic, and electronic features of a new group of functionalized MXenes, Mo_2MC_2X (M = Mn, W; X = O_2, S_2, OS). The materials' stability has been confirmed by formation energy and the analysis of the Born criteria. To further understand the other mechanical properties of these materials, Poisson's ratio ν, Young's modulus Y and the Shear modulus G were calculated and checked against other 2D materials. The mechanical property calculations confirm the exceptional mechanical flexibility of functionalized MXenes. Eventually, the electronic band calculation results show that all MXenes are metallic.

Acknowledgments

The authors acknowledge TUBITAK ULAKBIM, High Performance and Grid Computing Center (TRUBA resources) for providing computational time.

Conflict of Interest

The authors declare there are no conflicts.

REFERENCES

1. Xiao, B.; Li, Y.C.; Yu, X.F.; Cheng, J.B. Sens. Actuat. B-Chem. **2016**, 235, 103.

2. Chen, J.; Chen, K.; Tong D.; Huang, Y.; Zhang, J.; Xue, J. Chem. Commun. **2015**, 51, 314.

3. Lukatskaya, M.R.; Mashtalir, O.; Ren, C.E.; Dall'Agnese, Y.; Rozier, P.; Taberna, P.L. Science **2013**, 341, 1502.

4. Reunchan, P.; Jhi, S.H. Appl. Phys. Lett. **2011**, 98, 093103.

5. Tang, Q.; Zhou, Z.; Shen, P.W. J. Am. Chem. Soc. **2012**, 134, 16909.

6. Anasori, B.; Lukatskaya, M.R.; Gogotsi, Y. Nat. Rev. Mater. **2017**, 2, 16098.

DOI: http://dx.doi.org/10.32571/ijct.1661831 **E-ISSN: 2602-277X**

7. Hu, Q.K.; Wang, H.Y.; Wu, Q.H.; Ye, X.T.; Zhou, A.G.; Sun, D.D. Int. J. Hydrogen Energy **2014**, 39, 10606

8. Hu, Q.K.; Sun, D.D.; Wu, Q.H.; Wang, H.Y.; Wang, L. B.; Liu, B.Z. J. Phys. Chem. A **2013**, 117, 14253-14260.

9. Ling, C.; Shi, L.; Ouyang, Y.; Chen, Q.; Wang, J. Adv. Sci. **2016**, 3, 1600180.

10. Guo, Z.; Miao, N.; Zhou, J.; Sa, B.; Sun, Z. J. Mater. Chem. C **2017**, 5, 978.

11. Yang, J.; Luo, X.; Zhang, S.; Chen, L. Phys. Chem. Chem. Phys. **2016**, 18, 12914.

12. Yang, J.; Zhou, X.; Luo X.; Zhang, S. Chen L. Appl. Phys. Lett. **2016**, 109, 203109.

13. Yang, J.; Luo, X.; Zhou, X.; Zhang, S.; Liu, J.; Xie, Y. Comput. Mater. Sci. 2017, 139, 313-319.

14. Zhang, L.; Qu, X; Lu., S.; et al. Int J Hydrogen Energy **2022**, 47, 4211e21.

15. Hu, T.; Li, Z.; Hu, M.; Wang, J.; Hu, Q.; Li Q.; Wang, X. J. Phys. Chem. C **2017**, 121, 19254–19261.

16. Li, L. Comput. Mater. Sci. **2016**, 124, 8–14.

17. Anasori, B.; Lukatskaya, M.R.; Gogotsi, Y. Nat Rev Mater 2017, 2, 16098.

18. Alhabeb, M.; Maleski, K.; Anasori, B.; et al. Chem Mater. **2017**, 29, 7633e44.

19. Hu, M.; Hu, T.; Li, Z., et al. ACS Nano **2018**, 12, 3578e86.

20. Kamysbayev, V.; Filatov, AS.; Hu, H.; Rui, X.; Lagunas, F.; Wang, D.; Klie, R.F.; Talapin, D.V. Science, **2020**, 369, 979–983.

21. Weng, H.; Ranjbar, A.; Liang, Y.; Song, Z.; Khazaei, M.; Yunoki, S.; Arai, M.; Kawazoe, Y.; Fang, Z.; Dai, X. Phys. Rev. B: Condens. Matter Mater. Phys., **2015**, 92, 075436.

22. Fashandi, H.; Ivady, V.; Eklund, P.; Spetz, A.L.; Katsnelson, M.I.; Abrikosov, I.A. Phys. Rev. B: Condens. Matter Mater. Phys., **2015**, 92, 155142.

23. Bai, Y.; Zhou, K.; Srikanth, N.; Pang, J.H.; He, X.; Wang, R. RSC Adv., **2016**, 6, 35731–35739.

24. Khazaei, M.; Ranjbar, A.; Arai, M.; Sasaki, T.; Yunoki, S. J. Mater. Chem. C, **2017**, 5, 2488–2503.

25. Zha, XH.; Zhou, J.; Zhou, Y.; Huang, Q.; He, J.; Francisco, J.S.; Luo, K.; Du, S. Nanoscale, **2016**, 8, 6110-6117.

26. Eames, C.; Islam, M.S. J. Am. Chem. Soc., **2014**, 136, 16270–16276.

27. Zhang, J.; Jia, S.; Kholmanov, I.; Dong, L.; Er, D.; Chen, W.; Guo, H.; Jin, Z.; Shenoy, V.B.; Shi, L. ACS Nano, **2017**, 11, 8192–8198.

28. Bölen, E. Boron **2024**, 9(3), 129 – 134.

29. Zhu, J.; Chroneos, A.; Eppinger, J.; Schwingenschlögl, U. Appl. Mater. Today, **2016**, 5, 19-24.

30. Li, Y.M.; Guo, Y.L.; Jiao, Z.-Y. Curr. Appl. Phys., **2020**, 20, 310–319.

31. Anasori, B.; Xie, Y.; Beidaghi, M. ACS Nano **2015**, 9, 9507.

32. Hong, W.; Wyatt, B.C.; Nemani, S.K.; Anasori, B. MRS Bull **2020**, 45, 850.

33. Wang, H.; Jing, Z.; Liu, H., et al. Nanoscale **2020**, 12, 24510.

34. Özcan, S.; Biel, B. Chem. Chem. Phys. **2023**, 25 (3), 1881–1888.

35. Lu, A.Y.; Zhu, H.; Xiao, J.; Chuu, C.P.; Han, Y.; Chiu, M.H.; Cheng, C.C.; Yang, C.W.; Wei, K.H.; Yang, Y.; et al. Nat. Nanotechnol. **2017**, 12, 744–749.

36. Wang, Y.; Wei, W.; Huang, B.; Dai, Y. Phys. Chem. Chem. Phys. **2019**, 21 (1), 70–76.

37. He, J.; Lyu, P.; Sun, L.Z.; Garcia, A.M.; Nachtigall, P. J. Mater. Chem. C **2016**, 4, 6500–6509.

38. Liu, M.-Z.; Li, X.-H.; Cui, X.-H.; Zhang, R.-Z.; Cui, H.-L. Vacuum **2023**, 215, 112373.

39. Kresse, G.; Hafner, J. Phys Rev B, **1993**, 47, 558–561.

40. Kresse, G.; Hafner, J. Phys Rev B, **1994**, 49, 14251–14269.

41. Kresse, G.; Furthmüller, J. Comput Mater Sci 1996, 6, 15–50.

42. Kresse, G.; Furthmüller, J. Phys Rev B **1996**, 54, 11169–11186.

43. Kresse, G.; Joubert, D. Phys Rev B **1999**, 59, 1758–1775.

DOI: http://dx.doi.org/10.32571/ijct.1661831 **E-ISSN: 2602-277X**

44. Blöchl, P.E. Phys Rev B **1994**, 50, 17953–17979.

45. Perdew, J.P.; Burke, K.; Ernzerhof, M. Phys. Rev. Lett., **1996**, 77, 3865–3868.

46. Perdew, J.P.; Zunger, A. Phys. Rev. B: Condens. Matter Mater. Phys., **1981**, 23, 5048-5079.

47. Monkhorst, H.; Pack, J. Phys. Rev. B: Solid State, **1976**, 13, 5188-5192.

48.Page, Y.L.; Saxe, P. Phys. Rev. B: Condens. Matter Mater. Phys., **2002**, 65, 104104.

49. Li, N.; Zeng, Z.; Zhang, Y.; Chen, X.; Kong, Z.; Arramel, Li Y.; Zhang, P.; Nguyen, B.S. ACS Omega **2021**, 6, 23676−23682.

50. Born, M. Proc. Cambridge Philos. Soc. **1940**, 36, 160–172.

51. Thoma, S.; Ajith, K.M.; Lee, S.; Valsakumar, M.C. RSC Adv. **2018**, 8, 27283-27292.

52. Wei, X.; Fragneaud, B.; Marianetti, C.A.; Kysar, J.W. Phys. Rev. B: Condens. Matter Mater. Phys., **2009**, 80, 205407.

53. Andrew, R.C.; Mapasha, R.E.; Ukpong, A.M.; Chetty, N. Phys. Rev. B: Condens. Matter Mater. Phys., **2012**, 85, 125428.

54. Çakır, D.; Peeters, F.M.; Sevik, C. Appl. Phys. Lett., **2014**, 104, 203110.

55. John, R.; Merlin, B. Theory Appl., **2016**, 5, 43–55.

56. Geng, J.; Rucheng, W.; Haoyun, B.; Iat-Neng, C.; Kar, W.N.; Weng, F.I.; Hui, P. International journal of hydrogen energy **2024**, 7, 18725-18737.